Journal of ELECTRONIC MATERIALS, Vol. 39, No. 4, 2010
DOI: 10.1007/s11664-010-1119-2

Electrical Properties of $Ca_9ZnLi(PO_4)_7$ Ceramics Prepared by Reactive Pressureless Sintering

DONGLEI WEI,[1] YANLIN HUANG,[1] JIN SOO KIM,[2] LIANG SHI,[2] and HYO JIN SEO[2,3]

1.—College of Chemistry, Chemical Engineering, and Materials Science, Soochow University, Suzhou 215123, China. 2.—Department of Physics, Pukyong National University, Busan 608-737, Republic of Korea. 3.—e-mail: hjseo@pknu.ac.kr

Well-crystallized $Ca_9ZnLi(PO_4)_7$ ceramics were prepared by reactive pressureless sintering at atmospheric pressure. The single-phase $Ca_9ZnLi(PO_4)_7$ ceramics were confirmed by x-ray diffraction (XRD). The dielectric and electrical properties were investigated over a wide frequency range (1 Hz to 1 MHz) by complex impedance spectroscopy at different temperatures between 25°C and 600°C. A dielectric anomaly was observed at 440°C, which might be related to the phase transition. The impedance Cole–Cole plot was used to analyze the results of complex impedance measurements, revealing that the electrical properties depend strongly on frequency and temperature. Two relaxation dispersions of the electrical parameters were found and analyzed in terms of bulk and grain-boundary ionic transfer processes. The slope of the alternating-current (AC) conductivity over a wide range of temperatures provides activation energies from 0.48 eV to 1.69 eV. These results suggest that the conduction process is of the mixed type.

Key words: Phosphate, ceramics, pressureless sintering, dielectric properties

INTRODUCTION

Tricalcium phosphates [TCP, $Ca_3(PO_4)_2$] are attractive materials for biologists, mineralogists, and inorganic and industrial chemists.[1] β-$Ca_3(PO_4)_2$ is preferred as a bioceramic on account of its chemical stability, mechanical strength, and proper bioresorption rate.[2] β-$Ca_3(PO_4)_2$-type compounds (space group *R3c*) have six Ca sites. The Ca(1), Ca(2), and Ca(3) sites are in eightfold coordination, the distorted octahedral Ca(5) site is fully occupied by Ca^{2+} ions, the Ca(4) site surrounded by nine O atoms is 50% occupied by Ca^{2+} ions, and the Ca(6) site is vacant.[3] This special crystal structure permits rich heterovalent substitutions to occupy or form vacancies in the structure,[4–6] for example, $3Ca^{2+} \rightarrow 2R^{3+} + \square$ [R^{3+} = rare earth (RE), Y, Fe, Al],[7] $3Ca^{2+} + \square \rightarrow R^{3+} + 3M^{+}$, or $Ca^{2+} + \square \rightarrow 2M^{+}$ (M = Li, Na, K) ($\square$ = vacancy).[6]

A variety of compounds with the β-$Ca_3(PO_4)_2$ structure have been reported in the literature, for example, $Ca_9A'A''(PO_4)_7$ (A″ = Li, Na, K; A′ = Mg, Ca, Mn, Co).[8–13] Teterskii et al.[14] have investigated dielectric and second-harmonic generation (SHG) for the whitlockite solid solutions $Ca_{9-x}M_xR(PO_4)_7$ (x = 1, 1.5; M = Mg, Zn, Cd; R = Ln, Y). The conductivity and transition temperature in the calcium-ion solid electrolyte $Ca_{9-x}M_xR(PO_4)_7$ have also been investigated at different temperatures. These materials preserve a polar whitlockite-type crystal structure and served as the basis for crystallochemical design of compounds with ferroelectric, nonlinear optical, and ion-conductive properties.[14,15] Many compounds with the whitlockite structure have been reported in the literature. Among the triple phosphates, antiferroelectric properties have been studied only for $Ca_{9-x}M_xR(PO_4)_7$ (x = 1, 1.5; M = Mg, Zn, Cd; R = Ln, Y).[14] However,

(Received June 8, 2009; accepted February 6, 2010; published online March 4, 2010)

investigation of the electrical properties of β-$Ca_3(PO_4)_2$ is limited to date.

The purpose of this work is to synthesize the $Ca_9ZnLi(PO_4)_7$ ceramics on the basis of the whitlockite-like structure and investigate their electrical properties. $Ca_9ZnLi(PO_4)_7$ ceramics were prepared by reactive pressureless sintering under air atmosphere. The frequency dependence of the dielectric constant and the AC conductivity as a function of temperature have been measured. Conduction processes analyzed by impedance Cole–Cole plot are discussed according to the contributions of the bulk and grain boundaries, and the interfacial effect.

EXPERIMENTAL PROCEDURES

The $Ca_9ZnLi(PO_4)_7$ ceramics were synthesized by the conventional reaction-sintering process. The starting material was a stoichiometric mixture of reagent-grade $CaCO_3$, ZnO, $(NH_4)_2HPO_4$, and Li_2CO_3. Firstly, the mixture was heated to 350°C and kept at this temperature for 6 h. Secondly, the powders were mixed again and heated at 700°C for 6 h. The obtained powders were thoroughly mixed in acetone. Thirdly, the powder without any pressure was then heated to 900°C and kept at this temperature for 15 h in air. After that, the temperature was slowly decreased to 700°C in 15 h to 20 h and then quenched to room temperature (RT). A dense ceramics with ρ = 2.873 g/cm^3 was obtained.

XRD patterns were collected by using a Rigaku D/Max diffractometer operating at 40 kV, 30 mA with Bragg–Brentano geometry using Cu K_α radiation (λ = 1.5405 Å). The grain morphology of the ceramics was investigated by using a JEOL-5600 scanning electron microscope (SEM).

Round pellets were cut from the $Ca_9ZnLi(PO_4)_7$ ceramics. To investigate the electrical properties, a Pt electrode was coated on the pellet surface by direct-current (DC) sputtering. The dielectric and electrical properties were investigated by using an impedance analyzer (HP4194A).

RESULTS AND DISCUSSION

Crystalline Phase and Grain Morphology

Figure 1 shows the XRD pattern of $Ca_9ZnLi(PO_4)_7$ ceramics. It is found that the pattern is well consistent with JCPDS card no. 50-0339. This indicates that the ceramics were crystallized into a single-phase component. No impurity peak was observed in the XRD pattern. All the reflections could be well indexed to the whitlockite-type hexagonal structure of β-$Ca_3(PO_4)_2$ with the *R3c* space group.

Figure 2 shows an SEM micrograph of $Ca_9ZnLi(PO_4)_7$ ceramics. The ceramics consist of closely packed grains. Furthermore, the surface of the grains was smooth, indicating that well-crystallized $Ca_9ZnLi(PO_4)_7$ ceramics could be obtained by reactive pressureless sintering under an air atmosphere.

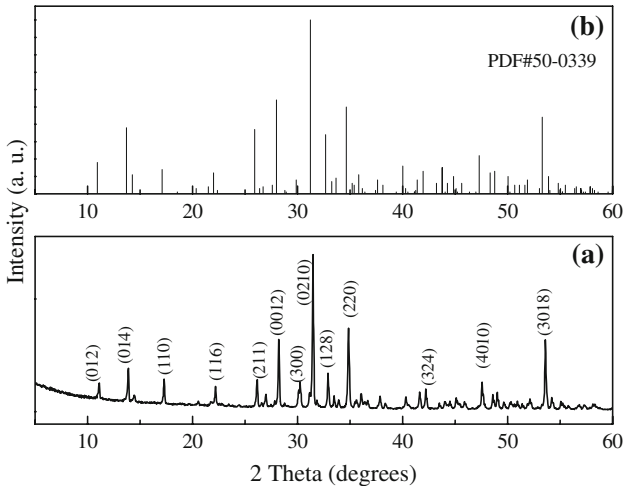

Fig. 1. XRD patterns of $Ca_9ZnLi(PO_4)_7$ ceramics (a) and PDF card no. 50-0339 (b).

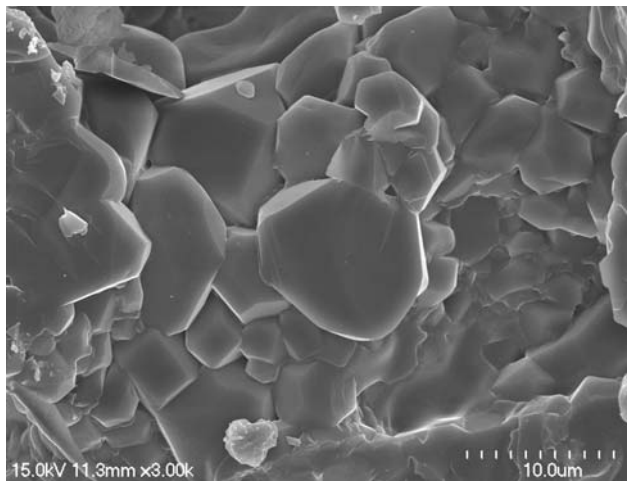

Fig. 2. SEM image of the surface of $Ca_9ZnLi(PO_4)_7$ ceramics.

Dielectric Properties of $Ca_9ZnLi(PO_4)_7$ Ceramics

Figure 3a presents the real dielectric constant of $Ca_9ZnLi(PO_4)_7$ ceramics measured at 10 Hz, 100 Hz, 1 kHz, 10 kHz, and 100 kHz. The dielectric constant increases smoothly with increasing temperature. A dielectric anomaly is observed at 440°C, indicating that a phase transition occurs at this temperature. On the other hand, the value of the dielectric constant above 250°C depends on the measurement frequency. Thus the ceramics exhibit strong low-frequency dielectric dispersion. In addition, dielectric loss showed obvious increases above 250°C (Fig. 3b). The ions could be activated by increasing the thermal energy by elevating the temperature, thus the low-frequency dielectric dispersion is caused by ionic charge carriers resulting in increased dielectric loss.

In the whitlockite-type hexagonal structure, a structural phase transition from space group *R3c* to

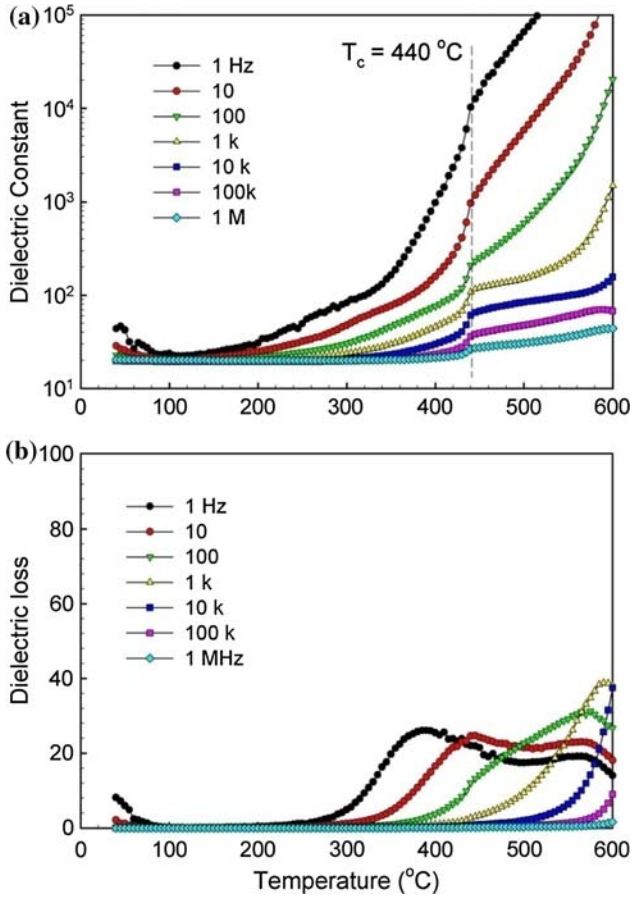

Fig. 3. The dependence of dielectric constant (a) and dielectric loss (b) of the $Ca_9ZnLi(PO_4)_7$ ceramics on temperature at different frequencies.

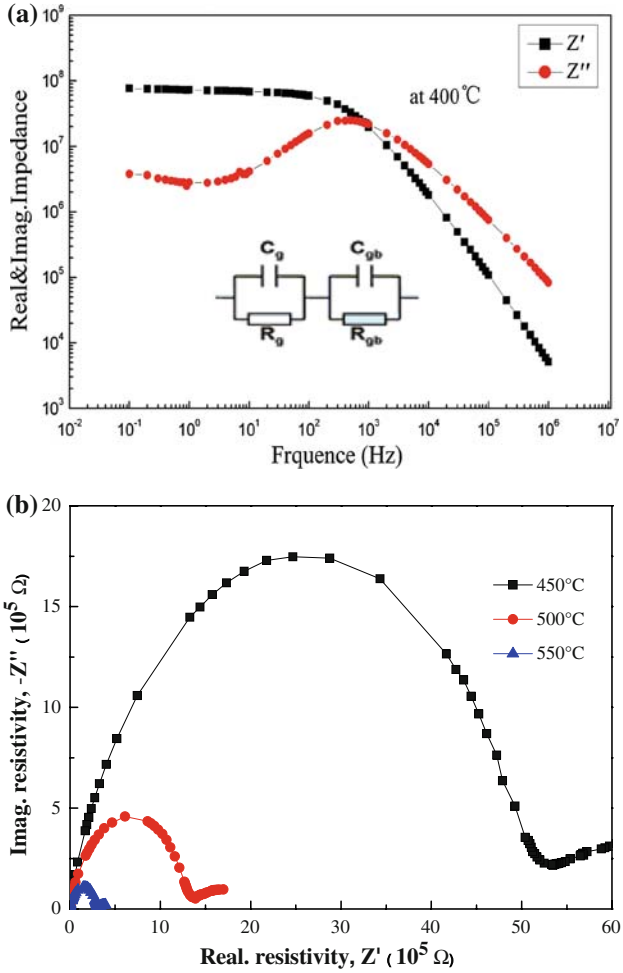

Fig. 4. Real and imaginary impedance and frequency responses for the $Ca_9ZnLi(PO_4)_7$ ceramics at 400°C (a); and the impedance Cole–Cole plot at selected temperatures (b).

$R\bar{3}c$ is possible.[16] Lazoryak et al.[17] have reported this kind of phase transition in $Ca_9Fe(PO_4)_7$ (at 890 ± 10 K) with the whitlockite-type crystal structure. The dielectric measurements reveal the ferroelectric nature of the phase transition.[17] In $Ca_3(VO_4)_2$-$LaVO_4$ cation conductors, partial La^{3+} substitution in $Ca_{3-x}La_{2x/3}(VO_4)_2$ $(0 \le x \le 1)$ (whitlockite-like structure) noticeably reduces the temperature of the polymorphic transition.[18] So, it can be speculated that, when Zn^{2+} and Li^+ ions are doped into β-$Ca_3(PO_4)_2$, the phase-transition temperature (710 ± 10 K) could also be reduced. The dielectric anomaly in the $Ca_9ZnLi(PO_4)_7$ ceramics could be tentatively assigned to a structural phase transition. However, the unit-cell dimensions do not have an obvious change in this type of phase transition from $R3c$ to $R\bar{3}c$.[17]

Impedance Spectroscopy

Usually, the electrical contribution of the grains and grain boundaries are described by the complex impedance plot from impedance spectroscopy. Especially, the impedance Cole–Cole plot can be expressed by a modified Debye expression:

$$Z^*(\omega) = \frac{z_0}{1 + (i\omega\tau_0)^n}\left(\tau_0 = \frac{1}{\omega_0} = \frac{1}{2\pi f_\gamma}\right), \qquad (1)$$

where ω_0 is the relaxation angular frequency ($\omega = 2\pi f$), τ_0 is the mean relaxation time, and the factor n takes values over the range $0 \le n \le 1$. If the factor n is unity then the relaxation process is a Debye-type process with a single relaxation time.

Figure 4a shows the frequency dependence of the real (Z') and imaginary part (Z'') of the complex impedance at 400°C. The real impedance (Z') decreases while the imaginary (Z'') impedance exhibits a peak with increasing frequency, indicating impedance relaxation. This impedance relaxation could be due to the ionic conduction process. However, the complex plot exhibits a semicircular arc in Fig. 4b, which is described by a Debye-like Cole–Cole relaxation with a single relaxation time.[19]

Calculations of x-ray diffraction patterns and second-harmonic generation tests on $Ca_{9-x}M_xR(PO_4)_7$, (M = Zn^{2+}, Mg^{2+}, Cd^{2+}) also confirmed that M^{2+}

cations first occupied the octahedrally coordinated cation position Ca(5), and only after fully occupying this position entered the other less favorable positions.[14] So, it could be suggested that Zn^{2+} cations prefer to occupy Ca(5) sites in $Ca_9ZnLi(PO_4)_7$.

In the whitlockite-type structure, alkali-metal cations occupy two close positions, $M(4_1)$ and $M(4_2)$, both statistically and nonequivalently.[20] Nonequivalent filling of two close positions observed earlier for a-$Na_3Sc_2(PO_4)_3$ results in the appearance of ferroelectric properties in these crystals.[21] In the $Ca_9MgLi(PO_4)_7$ structure, lithium cations occupy two positions, Li(1) and Li(2), in the $M(4_1)O_6$ and $M(4_2)O_6$ octahedra, respectively.[22] The lithium cations in position M(4) start migrating from one site to another with changing temperature.[23] The structural aspects of Ca^{2+} mobility in whitlockite structures were addressed in Ref. 24. In $Ca_9ZnLi(PO_4)_7$, the Ca^{2+} and Li^+ ions both participate in the process of conductivity, which may be a kind of complex conductor.

The variation of Z' with Z'' (Cole–Cole plot) for $Ca_9ZnLi(PO_4)_7$ ceramics at different temperatures is shown in Fig. 4b, exhibiting two impedance arcs in two separate frequency ranges. This suggests that two different conduction mechanisms are present in the measured frequency and temperature range. The semicircle in the high-frequency region is representative of the bulk properties of grains. The centers of the impedance semicircles lie below the real axis. Another impedance arc in the low-frequency region is related to the grain boundaries.

Electrical Conductivity

The frequency variation of the AC conductivity, $\sigma(\omega)$, at various temperatures is shown in Fig. 5. There is an increase in AC conductivity followed by a frequency-independent plateau region at high temperatures. At low temperatures, $\sigma(\omega)$ increases with increasing frequency, which is characteristic of the power-law dependence, ω^s (s = exponential). However, $\sigma(\omega)$ at high temperatures and low frequencies shows a flat (plateau) response. It has been well described by Almond et al.[25,26] that this response is typical of a resistor–capacitor microstructure network. The low-frequency plateau is dominated by conduction through the conductive region and frequency-dependent region, whereas as at higher frequency it is due to AC conductivity through the dielectric region. As temperature increases the low-frequency conductivity increases and dominates the curve.[25,26] The nature and mechanism of the conductivity dispersion in solids are generally analyzed using Jonscher's power law; $\sigma(\omega) = \sigma_0 + A\omega^s$, where σ_0 is the DC conductivity in a particular range of temperature, A is a temperature-dependent parameter, and s is the temperature-dependent exponent, which falls in the range $0 \le s \le 1$. The exponent s represents the degree of interaction between mobile ions with the lattices

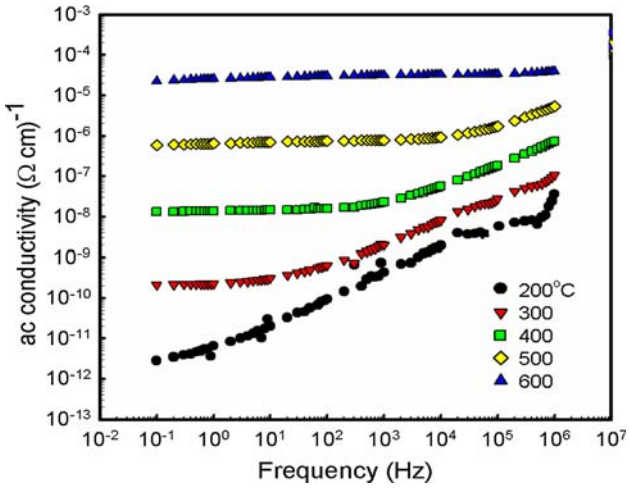

Fig. 5. The variation of σ_{AC} as a function of frequency at different temperatures.

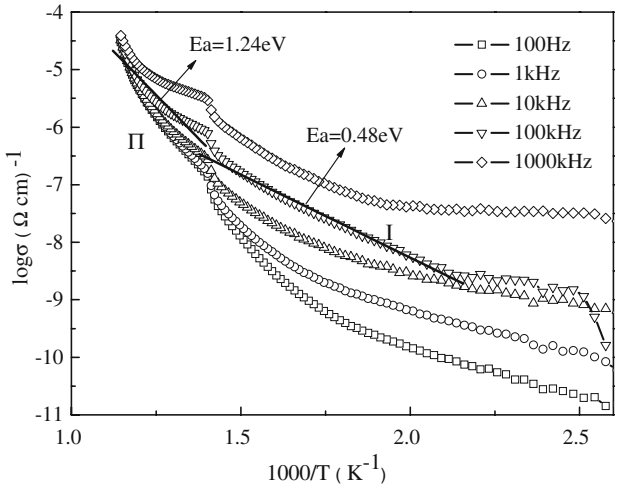

Fig. 6. Variation of σ_{AC} as a function of temperature at different frequencies.

around them, and the prefactor exponent A determines the strength of polarizability.

The temperature dependence of the AC conductivity, σ_{AC} measured at different frequencies is shown in Fig. 6. The frequency dependence of the AC conductivity tends to merge with increasing temperature. The AC conductivity is described by an Arrhenius relation:

$$\sigma(T) = \sigma_0 \exp\left(\frac{-Ea}{kT}\right), \qquad (2)$$

where E_a is the activation energy and k is the Boltzmann constant. The electrical conductivity is dominant by intrinsic defects above 200°C. The activation energies were calculated at different temperatures and are listed in Table I.

It is clear that the activation energy increases at elevated temperatures. For example, the activation energy at 100 kHz was estimated to be 1.24 eV in

Table I. Comparison of activation energy of different regions

Frequency (kHz)	Regions	E_a (eV)
0.1	*I*	1.69
	II	1.03
1	*I*	1.66
	II	0.78
10	*I*	1.67
	II	0.49
100	*I*	1.24
	II	0.48
1000	*I*	0.75
	II	0.58

the high-temperature region and 0.48 eV in the low-temperature region. The activation energy may be attributed to calcium ion hopping, similar to that in calcium-ion solid solutions of $Ca_3(VO_4)_2$-$LaVO_4$ in the whitlockite-like structure.[18] It was shown that there were two types of continuous paths for the interstitial-like mechanism of Ca^{2+} transport in $Ca_3(VO_4)_2$ and related solid solutions: … → M(4) → M(2) → M(4′) → … (path I) and … → M(4) → M(3) → M(6) → M(3′) → M(4′) → … (path II). According to the structural data, Ca may pass from an M(2) site to an empty M(4) site and then follow path I.

Another possibility is the transition from M(3) to M(4′) and M(6) vacancies and then along path II. These migration paths can be called a vacancy mechanism of transport.[24] Thus, calcium ion hopping may be responsible for the conduction process with increasing temperatures. On the other hand, an abnormal change of the slope in the vicinity of T_c = 440°C can also be observed in the dielectric anomaly in Fig. 3a.

Zn and Li ions can easily substitute for Ca ions with increasing temperature. This could change the type of continuous paths for the interstitial-like mechanism of Ca^{2+} transport in β-$Ca_3(PO_4)_2$. So, the activation energy of $Ca_9ZnLi(PO_4)_7$ was found to increase noticeably with increasing temperature. The activation energy is low in the low-temperature range. These low values of activation energy suggest that a small amount of energy is required to activate the carriers for electrical conduction. However, the conduction process with E_a = 1.24 eV is possible in the high-temperature range. Thus, calcium ion hopping may be responsible for the conduction process at high thermal energy.

CONCLUSIONS

$Ca_9ZnLi(PO_4)_7$ ceramics have been successfully fabricated by reactive pressureless sintering. Formation of a single phase was confirmed by XRD. The temperature dependences of the dielectric constant exhibited a strong low-frequency dielectric dispersion above 250°C due to the contribution by charge carriers. Impedance relaxation is observed as a semicircular arc and described by a Debye-like Cole–Cole relaxation. The AC conductivity $\sigma(\omega)$ increases with the elevated frequency, which is a characteristic of the power law: $\sigma(\omega) = \sigma_0 + A\omega^s$. The temperature dependence of the AC conductivity shows a change at about 440°C, corresponding to the anomaly in the dielectric constant. The activation energy was estimated to be 1.24 eV in the high-temperature region and 0.48 eV in the low-temperature region, which is attributed to calcium ion hopping. These results suggest that the conduction process is of the mixed type.

ACKNOWLEDGEMENTS

This work was financially supported by a Korea Science and Engineering Foundation (KOSEF) Grant funded by the Korean government (MEST) (No. 2009-0078682).

REFERENCES

1. M. Yashima, A. Sakai, T. Kamiyama, and A. Hoshikawa, *J. Solid State Chem.* 175, 272 (2003).
2. R. Famery, N. Richard, and P. Boch, *Ceram Int.* 20, 327 (1994).
3. A.A. Belik, F. Izumi, T. Ikeda, M. Okui, A.P. Malakho, V.A. Morozov, and B.I. Lazoryak, *J. Solid State Chem.* 168, 237 (2002).
4. H.G. Shaeken and F.C.M. Driessens, *Z. Anorg. Allg. Chem.* 505, 48 (1983).
5. B.I. Lazoryak, S.V. Khoina, and V.N. Golubev, *Sov. Zh. Inorg. Chem.* 35, 1373 (1990).
6. B.I. Lazoryak, T.V. Strunenkova, V.N. Golubev, E.A. Vovk, and L.N. Ivanov, *Mater. Res. Bull.* 31, 207 (1996).
7. B.I. Lazoryak, V.N. Golubev, R. Salmon, C. Parent, and P. Hagenmuller, *Eur. J. Solid State Inorg. Chem.* 26, 455 (1989).
8. C. Calvo and R. Gopal, *Am. Mineral.* 60, 120 (1975).
9. B.I. Lazoryak, *Russ. Chem. Rev.* 65, 307 (1996).
10. V.A. Morozov, I.A. Presnyakov, A.A. Belik, S.S. Khasanov, and B.I. Lazoryak, *Crystallogr. Rep.* 42, 758 (1997).
11. V.A. Morozov, A.A. Belik, R.N. Kotov, I.A. Presnyakov, S.S. Khasanov, and B.I. Lazoryak, *Crystallogr. Rep.* 45, 13 (2000).
12. A.A. Belik, V.B. Gutan, L.N. Ivanov, and B.I. Lazoryak, *Russ. J. Inorg. Chem.* 46, 785 (2001).
13. A.A. Belik, V.A. Morozov, S.S. Khasanov, and B.I. Lazoryak, *Mater. Res. Bull.* 34, 883 (1999).
14. A.V. Teterskii, S.Yu. Stefanovich, B.I. Lazoryak, and D.A. Rusakov, *Russ. J. Gen. Chem.* 52, 308 (2007).
15. A.L. Mackay and D.P. Sinha, *J. Phys. Chem. Solids* 28, 1337 (1967).
16. M.E. Lines and A.M. Glass, *Principles and Applications of Ferroelectrics and Related Materials* (Oxford: Clarendon, 1977).
17. B.I. Lazoryak, V.A. Morozov, and A.A. Belik, *Solid State Sci.* 6, 185 (2004).
18. I.A. Leonidov, O.N. Leonidova, L.L. Surat, and R.F. Samigullina, *Inorg. Mater.* 39, 616 (2003).
19. J.R. Dygas, *Solid State Ionics* 176, 2065 (2005).
20. V.A. Efremov and V.B. Kalinin, *Kristallografiya* 23, 703 (1978).
21. S.A. Okopenklo, S.Yu. Stefanovich, and V.B. Kalinin, *Fiz. Tverd. Tela (Leningrad)* 20, 2846 (1978).
22. V.A. Morozov, I.A. Presnyakov, A.A. Belik, S.S. Khasanov, and B.I. Lazoryak, *Crystallogr. Rep.* 42, 758 (1997).

23. V.A. Morozov, A.A. Belik, R.N. Kotov, I.A. Presnyakov, S.S. Khasanov, and B.I. Lazoryak, *Crystallogr. Rep.* 45, 13 (2000).
24. I.A. Leonidov, A.A. Belik, O.N. Leonidova, and B.I. Lazoryak, *Zh. Neorg. Khim*. 47, 357 (2002).
25. C.R. Bowen and D.P. Almond, *Mater. Sci. Technol.* 22, 719 (2006).
26. D.P. Almond, C.R. Bowen, and D.A.S. Rees, *J. Phys. D Appl. Phys.* 39, 1295 (2006).